The Role of Quantum Interference in Intramolecular Singlet Fission

Kaia R. Parenti[1], Rafi Chesler[2], Guiying He[4,5], Pritam Bhattacharyya[6], Beibei Xiao[8], Daniel Malinowski[1], Jocelyn Zhang[1], Xiaodong Yin[8], Alok Shukla[7], Sumit Mazumdar[2,3]*, Matthew Y. Sfeir[4,5]*, Luis M. Campos[1]*

[1]Department of Chemistry, Columbia University, New York, New York 10027, USA

[2]Department of Physics, University of Arizona, Tucson, Arizona 85721, USA

[3]Department of Chemistry and Biochemistry, University of Arizona, Tucson, Arizona 85721, USA

[4]Department of Physics, Graduate Center, City University of New York, New York, New York 10016, USA

[5]Photonics Initiative, Advanced Science Research Center, City University of New York, New York, New York 10031, USA

[6]Institute for Theoretical Solid State Physics, Leibniz IFW Dresden, Helmholtzstr. 20, 01069 Dresden, Germany

[7]Department of Physics, Indian Institute of Technology Bombay, Powai, Mumbai 400076, India

[8]Key Laboratory of Cluster Science, Ministry of Education of China, Beijing Key Laboratory of Photoelectronic/Electrophotonic Conversion Materials, School of Chemistry and Chemical Engineering, Beijing Institute of Technology, Beijing 102488, P. R. China.

*mazumdar@email.arizona.edu

*msfeir@gc.cuny.edu

*lcampos@columbia.edu

Abstract

Quantum interference (QI), the constructive or destructive interference of conduction pathways through molecular orbitals, plays a fundamental role in enhancing or suppressing charge and spin transport in organic molecular electronics. Graphical models have been developed to predict constructive versus destructive interference in polyaromatic hydrocarbons, and have successfully estimated the large conductivity differences observed in single-molecule transport measurements. A major challenge lies in extending these models to excitonic (photoexcited) processes, which typically involve distinct orbitals with different symmetries. Here, we investigate how QI models can be applied as bridging moieties in intramolecular singlet fission (iSF) compounds to predict relative rates of triplet pair formation. In a series of bridged iSF dimers, we find that destructive QI always leads to slower triplet pair formation across different bridge lengths and geometries. A combined experimental and theoretical approach reveals the critical considerations of bridge topology and frontier molecular orbital energies in applying QI conductance principles to predict rates of multiexciton generation.

Introduction

Quantum interference (QI) effects have been invoked as an important mechanism to control charge/spin transport properties in molecular electronics.[1,2] For conduction pathways connected by alternant hydrocarbons, subtle variations in bond connectivity can impact conditions that lead to constructive or destructive quantum interference (CQI and DQI, respectively).[3,4] The classic example involves comparing transport between 1,3-phenylene (13Ph) and 1,4-phenylene (14Ph) bridges, where the conductance of the 13Ph bridge is decreased by several orders of magnitude due to DQI.[5,6] Graphical models have been established to predict molecular bridges that yield DQI and CQI as they pertain to phase-coherent charge transport through frontier molecular orbitals (FMOs) in conjugated systems.[7,8] This method involves drawing a continuous path from one connection point to the other, and pairing up atoms in the alternate path. If there is an odd number of atoms in the alternate path such that not all atoms are part of a pair, DQI is expected (**Figure 1**). A similar set of principles have been applied to biradical systems (Ovchinnikov's rule and related theorems) and used to predict the relative stabilities of the open-shell singlet and triplet states.[7,9]

The applicability of graphical QI models as a predictive tool for photoexcited (excitonic) processes in donor-bridge-acceptor (DBA) chromophores is less established. A key difference is that photoexcited charge transfer involves specific orbitals on donor and acceptor sites that may exhibit different symmetries compared to those involved in conductance measurements.[10] For example, Grozema and coworkers studied photoinduced electron and hole transfer in DBA chromophores. They found that QI could not be readily predicted from the connectivity of the bridge alone.[11] To explain differences in charge transfer rates for different bridge connectivity, it was necessary to also account for symmetry relations of the donor, bridge, and acceptor. These important fundamental results highlight the additional complexity inherent in describing dynamical photoexcited processes, which includes identifying key molecular orbitals and quantifying their character, relative energy, symmetries, and coupling strength. Computational modeling is thus essential to characterize QI effects in DBAs and other excited state systems.

More recently, bridged singlet fission chromophore systems have emerged as promising light-harvesting candidates for optoelectronic and chemical applications.[12–14] These intramolecular singlet fission (iSF) compounds exhibit long-lived multiexciton states (in the form of a coupled triplet pair) that extend over multiple chromophores. Studies have revealed the critical role of the

bridging unit (β) in modulating coupling between two (or more) singlet fission chromophores (SFCs) and dictating the rate of triplet pair formation and decay.[15–19] However, the impact of bridge connectivity on the SF dynamics in these systems has been largely excluded. The exception is a recent suggestion that bridge connectivity can modulate triplet pair binding energies, although this is only one consideration.[20,21] To date, there is no comprehensive model for applying QI concepts to multiexcitonic organic systems. Importantly, the platform of iSF systems offers versatility to study the role of QI, since covalent linkages and chromophores can be varied to access different conjugation and orbital symmetry patterns.[22] Furthermore, clear spectroscopic observables exist that allow for precise correlations to be made regarding the nature of QI and its influence on the rate of triplet pair formation. Defining the role of QI in SF would provide an important understanding of how bridge structure can be used to optimize electronic communication between SFCs and, more broadly, how conductance principles can be extended to multiexcitonic systems.

Here, we report how competing and coexisting QI effects drastically impact rates of triplet pair formation in bridged homodimers (SFC-β-SFC). We posit that graphical models of QI can be used to understand topological effects of bridging units in symmetric chromophores. To test this hypothesis, we use three alternant hydrocarbon bridges (phenylene, naphthalene, and anthracene) for which graphical models of QI patterns are well characterized.[8,23] **Figure 1** shows the predicted CQI (**14Ph**, **26N**, **15N**, and **26A**) and DQI (**13Ph**, **16N**, **27N**, and **27A**) structures for each bridge that links two pentacene or tetracene chromophores (**P$\boldsymbol{\beta}$P** and **T$\boldsymbol{\beta}$T**, respectively). We find that quantum interference effects can be predicted by graphical models in all compounds, with triplet pair formation being slower for any β that exhibits DQI. However, as we move from the smaller phenylene bridge to the larger naphthalene and anthracene bridges, we find that it is also important to consider other factors (including molecular geometry and resonance between SFC and bridge FMOs) to obtain a holistic picture of the SF rate constant. Importantly, we identify a distinct correlation between the strength of the charge transfer (CT) absorption resonances in the linear absorption spectra and the relative rates of iSF. These studies reveal the critical nature of chromophore connectivity in controlling the formation of the triplet pair, and the necessity of combined experimental and theoretical approaches to understand chemical design principles.

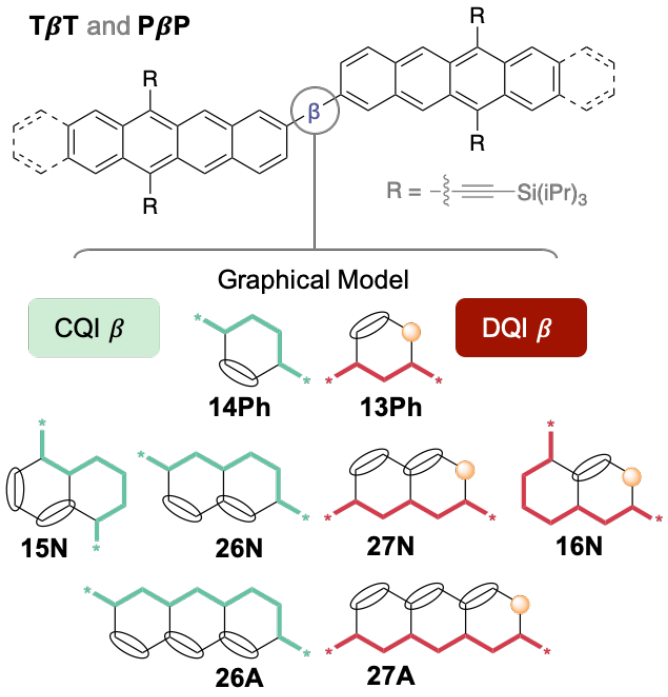

Figure 1. Model systems designed to investigate the role of quantum interference in pentacene and tetracene bridged dimers, **PβP** and **TβT**, where **β** = **14Ph**, **13Ph**, **15N**, **26N**, **27N**, **16N**, **26A**, and **27A**. The destructive quantum interference (DQI) bridging patterns (red) are expected to decrease the rate of singlet fission relative to the constructive quantum interference bridges (CQI, green).

Results and Discussion

We observe SF in all SFC-β-SFC compounds and find that the rate constants for triplet pair formation are markedly different for DQI connectivity, consistent with the graphical model (**Figure 1**). Importantly, QI-type effects persist across all bridges used in this study. In both pentacene and tetracene compounds (**PβP** and **TβT**), faster triplet formation is observed when β = **14Ph**, **26N**, and **26A**, compared to the corresponding DQI connectivity (β = **13Ph**, **27N**, and **27A**). This effect can be readily observed in the raw transient absorption data (**Figure 2a** and **Figure S2**) and single wavelength kinetics selective for the rise of the triplet (pentacene, **Figure 2b**) or decay of the singlet (tetracene, **Figure 2c**). Comparing **P-Ph-P** compounds, τ_{SF} drastically changes by a factor of 23, from 17 ps for **P-14Ph-P** to a much slower 391 ps for **P-13Ph-P**. This effect is even more pronounced in the analogous **T-Ph-T** compounds, with a faster τ_{SF} of 7 ps for **T-14Ph-T** to 65 times slower, 453 ps in **T-13Ph-T**. Significantly, DQI has a larger impact on the

singlet fission dynamics than proximity of the bridged **P** and **T** SFCs. For example, the rate of singlet fission in **13Ph** is ~ 2× slower than the previously reported 4,4'-biphenylene (β = **44bPh**) bridged compounds **P-44bPh-P** (τ_{SF} = 220 ps) and **T-44bPh-T** (τ_{SF} = 240 ps), which have double the bridge length.[24,25] This result underscores the significance of bridge connectivity in dictating triplet pair formation dynamics.

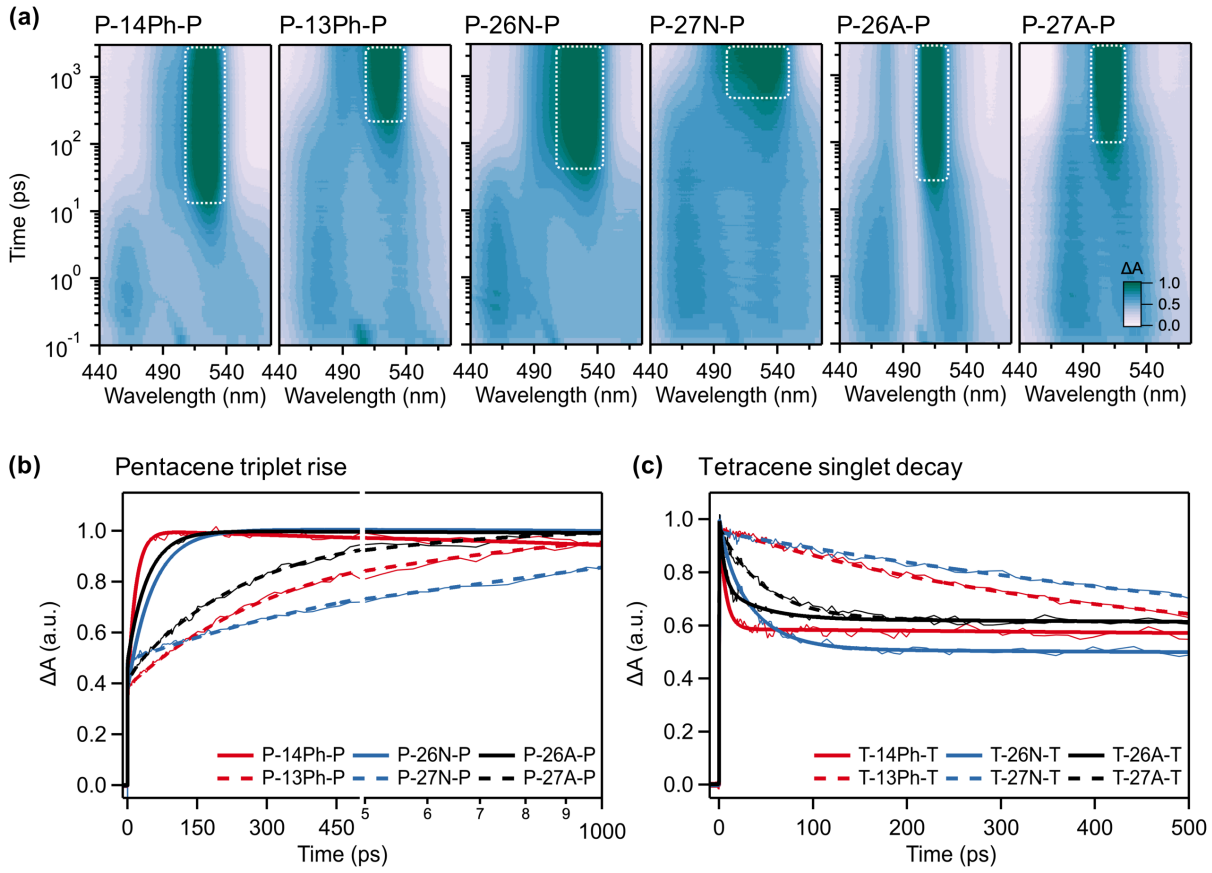

Figure 2. (a) Femtosecond transient absorption of pentacene compounds in dilute toluene solution (~50 μM) excited at 600 nm. Triplet photoinduced absorption is in green and outlined for clarity. Single wavelength kinetics corresponding to the rise of the pentacene triplet ~520 nm **(b)** and decay of the tetracene singlet ~455 nm **(c)** as a function of time.

Interestingly, we find that the magnitude of the difference between DQI and CQI effects diminishes with increasing bridge length, in the order of **Ph** > **N** > **A**. Analogous to **Ph** bridged compounds, large differences in the rate constants between DQI (**27N**) and CQI (**26N**) connectivity

points are observed in naphthalene bridged dimers. Triplet pair formation is slower in the **27N** DQI bridge relative to the **26N** CQI bridge by a factor of 16 in the pentacene series, and by a factor of 32 in the tetracene series. These differ in magnitude compared to the 23-fold/65-fold difference for **Ph** bridged compounds. Furthermore, triplet pair formation in the **27A** DQI bridge relative to the **26A** CQI bridge is a factor of 5 slower for **P$\boldsymbol{\beta}$P** and a factor of 4 slower for **T$\boldsymbol{\beta}$T**, a more subtle difference than what is observed for **Ph** and **N** bridges. A summary of iSF time constants for these compounds is shown in **Table 1**. The trends are depicted graphically in **Figure 3**, where the plots are normalized singlet fission rate as a function of chromophore, bridge type, and connectivity; and these are relative to the compound with the fastest rate of iSF in the series (**T-14Ph-T**). The monotonic decrease in the ratio of the rate of SF in CQI and DQI connectivity (k_{CQI}/k_{DQI}) is shown in **Figure 3**, where it is clear that tetracene chromophores exhibit a larger contrast in rate constants with the smallest bridge, but such difference decreases with the longer bridges.

Table 1. Rate and time constants for singlet fission in T$\boldsymbol{\beta}$T and P$\boldsymbol{\beta}$P.

β	TβT		PβP	
	k_{SF} (ps^{-1})	τ_{SF} (ps)	k_{SF} (ps^{-1})	τ_{SF} (ps)
14Ph	1.43×10^{-1}	7	5.95×10^{-2}	17
13Ph	2.21×10^{-3}	453	2.56×10^{-3}	391
26N	3.33×10^{-2}	30	1.80×10^{-2}	56
27N	1.05×10^{-3}	952	1.13×10^{-3}	882
15N	1.69×10^{-3}	591	9.50×10^{-4}	1053
16N	6.96×10^{-4}	1437	5.51×10^{-4}	1815
26A	7.14×10^{-2}	14	2.07×10^{-2}	48
27A	1.82×10^{-2}	55	3.96×10^{-3}	253

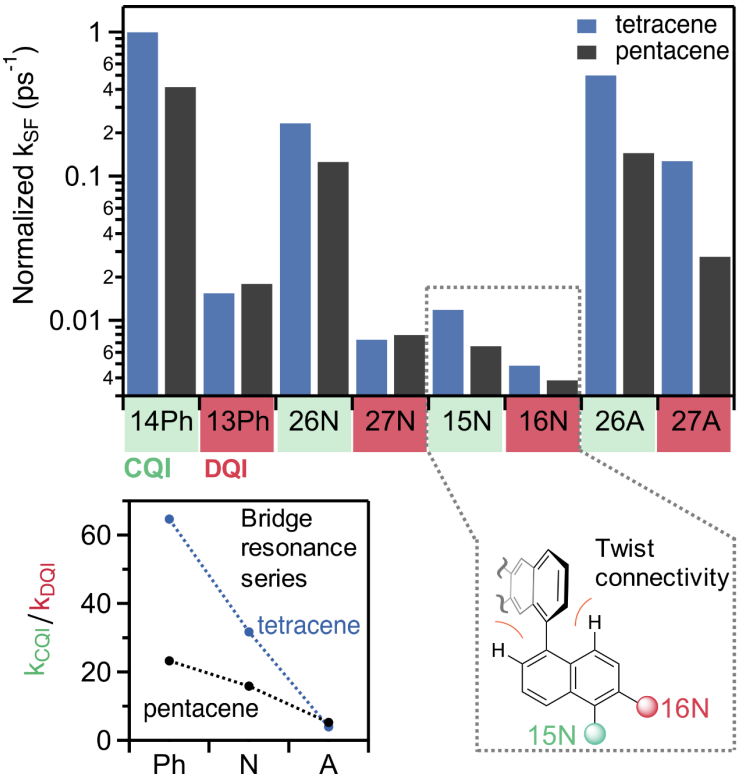

Figure 3. Comparison of SF rates (normalized to the largest k_{SF}) across all phenyl, naphthalene, and anthracene bridges in this work. Factors contributing to slow (fast) SF are boxed in red (green). Chromophores attached to the 1 and/or 5 positions of naphthalene exhibit larger dihedral angles than the 2, 6, or 7 positions, reducing overall planarity and slowing SF. Resonance between the frontier molecular orbitals of the anthracene bridge and SFC result in similar SF rates for CQI **26A** and DQI **27A** bridges.

The decrease in the contrast of the SF rate constants between CQI and DQI connectivity (k_{CQI}/k_{DQI}) is not correlated to an overall decrease in the absolute magnitude of k_{SF}. The anthracene bridge is notable in that, unlike other bridges, the DQI compounds exhibit relatively fast rates of singlet fission, though QI effects render them slower than the corresponding CQI compound. We have previously reported how the FMOs of the bridges impact the rates of SF, as observed in **T-26A-T** (τ_{SF} = 14 ps), **P-26A-P** (τ_{SF} = 48 ps), and others.[25] As the FMOs of the bridging units approach resonance with those of the SF chromophores, the rates of triplet pair formation are enhanced. Here, we find that this concept can also be extended to DQI bridge connectivity, such that moving from **P-13Ph-P** → **P-27N-P** → **P-27A-P** yields an initial increase in $\boldsymbol{\tau}_{SF}$ from 391 ps (**Ph**) to 882 ps (**N**) followed by a decrease to 253 ps (**A**). With these

considerations in mind, it can be reasoned that bridge resonance effects have a stronger impact on the anthracene-bridged DQI chromophores.[25,26] For example, the DQI chromophore **P-27A-P** undergoes faster iSF than **P-13Ph-P**, despite having a bridge that is longer by ~4.5 Å. Such a bridge resonance effect is even more pronounced in DQI tetracene analogs, where τ_{SF} is reduced by a factor of 17 from 952 ps (**27N)** to 55 ps (**27A**). While CQI compounds still undergo faster iSF (48 ps for **P-26A-P** and 14 ps in **T-26A-T**) than their DQI counterparts (253 ps in **P-27A-P** and 55 ps in **T-27A-T**), the difference between these two connectivities is much less drastic than within the phenyl and naphthalene systems (**Figure 3**).

Similar to how connectivity modulates bridge resonances effects, we have found that QI considerations must also be accounted for in the limit of large geometric distortions, which have been shown to greatly reduce chromophore-chromophore coupling.[27,28] For example, in **P-N-P,** density functional theory calculations indicate that chromophore attachment at the **1** and **5** positions are more twisted out of plane (~58°) than at the **2**, **6**, or **7** positions (~35°). This allows us to examine CQI and DQI in the highly twisted SFC couplings. We find that the β = **15N** CQI compounds undergo faster SF (1.05 ns in **P-15N-P** and 591 ps in **T-15N-T**) than the DQI analogues (1.8 ns in **P-16N-P** and 1.4 ns in **T-16N-T**, see **Figure S2**). We note that due to the QI effect, SF is actually faster in **15N,** where both chromophores are more twisted than in **16N**, where only one chromophore is highly twisted. These trends agree with simple graphical models, even though the overall singlet fission rates are relatively low due to overall weak chromophore-chromophore coupling. The effect of weak electronic coupling in the highly distorted **15N** connectivity has also been observed in single-molecule junction experiments.[29] These results imply that quantum interference remains a strong effect in the limit of both strong and weak interchromophore coupling.

While the above experimental observations highlight clear trends in the SF dynamics, they are not able to unambiguously identify the root causes of differences in the rate of triplet pair formation in DQI versus CQI compounds. For example, the triplet absorption spectra are not sharp enough to identify small differences in the electronic structures of the triplet pair for the two cases. Furthermore, these data are unable to assign the origin of the strong dependence of τ_{SF} on the length of the bridge molecule, i.e., even DQI compounds with anthracene bridge have unexpectedly fast SF. To capture these effects, we performed correlated-electron calculations of the excitonic states based on the π-electron only Pariser-Parr-Pople (PPP) model.[30,31] A key feature

of these calculations is that they include high order configuration interactions, which include quadruple excitations over a large active space (Methods and SI). Using this approach, we determine the wavefunctions and energies of (i) bright singlet states that are dominated by Frenkel exciton configurations localized on the SFC (denoted as LE_T, and LE_P for tetracene and pentacene, respectively) and bridge moieties (LE_β), (ii) eigenstates with contributions from charge transfer (CT) configurations between the SFC and bridge ($CT_{C\beta}$) as well as between the two SFCs (CT_{CC}), and (iii) the lowest triplet pair eigenstate $^1(TT)$.

These results show that the widely different τ_{SF} values between DQI and CQI compounds are not due to differences in their $^1(TT)$ wavefunctions. Instead, the calculated $^1(TT)$ eigenstate for all compounds is overwhelmingly dominated by triplet excitations occupying each of the terminal SFCs. Somewhat surprisingly, in all SF compounds excluding **14Ph** and **13Ph**, the $^1(TT)$ wavefunctions are nearly identical for all DQI and CQI compounds, independent of the bridge molecule. We show the three most dominant contributions to the $^1(TT)$ eigenstate common to **T-26N-T** and **T-27N-T** in **Figure 4a**. The near-complete $^1(TT)$ wavefunctions including configurations that make even smaller contributions are listed in **Figure S7** in the SI. Additional contributions to the wavefunctions beyond the dominant 2e-2h excitation (including 4e-4h excitations) are small, but taken together make nonnegligible contribution to the binding energy of $^1(TT)$.[32,33] Previous theoretical treatment suggested that the triplet pair states are fundamentally different for DQI vs CQI compounds.[21] Our calculations show that this result does not extend to bridges longer than β = **Ph**. As seen in **Figure S7** the $^1(TT)$ wavefunctions for a given SFC chromophore are nearly the same even with different bridge molecules.

It was also found that the contribution of optically allowed CT states to the excited state wavefunctions varies greatly with bridge connectivity and represents the determining factor for the singlet fission rate constant. In **T-26N-T** (**Figure 4b,c**) for example, the most dominant term in the wavefunction that contributes to the optical transition at ~3.5 eV is from a CT_{CC} configuration involving direct CT between the terminal tetracene molecules (**Figure 4b**). Interestingly, a similar charge transfer state also occurs in the DQI (**27N**) version of this compound, with the relative magnitudes of the largest amplitude terms being very similar to the CQI (**26N**) version. The primary difference between the two compounds is that the magnitude of the transition dipole moment between the ground state and the CT state is nearly zero in the DQI compound

(**27N**). This difference follows directly from the graphical model that predicts QI conditions: optical excitation within the PPP Hamiltonian conserves spin symmetry, and optically allowed CT processes can occur only between sites that are antiferromagnetically coupled. We have done detailed analyses of the correlated-electron exciton basis wavefunctions of the optically allowed excited states for all compounds (**Table 2**). The corresponding analysis for **P-26N-P** reveals an identical story.

We emphasize that there is a one-to-one correlation between the strength of the CT absorption and the relative magnitude of τ_{SF} between the DQI and CQI compounds with phenyl and naphthalene linkers. The experimental absorption spectra for short bridge lengths in the CT region agree strongly with the theory. In the CQI compounds (β = **14Ph**, **26N)**, we observe a single additional peak (absent in the monomer spectra) that is centered at 3 eV for **T$\boldsymbol{\beta}$T** (**Figure 4c** and SI) and 2.64 eV for **P$\boldsymbol{\beta}$P** (SI). In the corresponding DQI compounds (β = **13Ph**, **27N)**, this peak is largely absent. These differences reveal a quantum effect that is intimately related to the mechanism of SF. As has been previously recognized, the rate of transition from the singlet exciton to $^1(TT)$ can be enhanced by a virtual CT state.[34,35] The stronger the dipole coupling between the ground state and the CT state, the more easily it will be accessible as a virtual intermediate in a one-photon optical process. Furthermore, since the $^1(TT)$ in our dimers consists of triplets occupying only the terminal chromophores, fast τ_{SF} requires the virtual CT state to have significant contribution from configurations with direct CT between the terminal chromophores. The CT states in the CQI **T-26N-T** and **P-26N-P** satisfy both these criteria (**Table 2**) (τ_{SF} = 30 ps/56 ps). The corresponding states in DQI **T-27N-T** and **P-27N-P** either have weak dipole-coupling to the ground state or weak contributions from configurations with direct CT (τ_{SF} = 952 ps/882 ps). We note that when the energetics of singlet fission are satisfied, the strength of the CT transition in the linear absorption spectrum is directly correlated to the magnitude of the SF rate constant and can be used to predict relative rates of triplet pair formation.

The quantum effects that determine the SF rate with anthracene as the bridge molecule are more complex. The relatively small τ_{SF} in the DQI compounds here are ascribed to two competing quantum effects. First, the absence of long-range antiferromagnetic order in one dimension implies that, for long bridge molecules, spin couplings between distant atoms are not strictly antiferromagnetic or ferromagnetic.[36] As a result, CT between carbon atoms at the point of connectivity that would be forbidden from the graphical model of **Figure 1** can thus be optically

allowed. Second, this apparent deviation from the graphical model is accelerated by the proximity in the energies of the FMOs of the terminal chromophores and the bridge molecules (bridge resonance effect), which enhances quantum tunneling between the terminal chromophores. This is indeed what occurs in anthracene bridged SFCs, as the excited state wavefunctions of the optically allowed CT transitions contain significant bridge resonance contributions (**Table 2**). For example, in **T-26A-T** and **T-27A-T**, the relative weights of the three dominant constituents of the eigenstates at ~3.55 eV and ~3.75 eV, involve $CT_{C\beta}$, CT_{CC}, and LE_A with roughly equivalent amplitudes. Unlike the naphthalene case, the transition dipole couplings to these states in DQI **T-27A-T** is nonzero and only ~2-3 times smaller than the equivalent transition in the CQI **T-26A-T**. A qualitatively similar picture is observed in the eigenstates of **P-26A-P** and **P-27A-P**, with a slightly larger difference in the transition dipole couplings between CQI and DQI (~3-4 times smaller). These results explain our observation of only a ~4-5× change in τ_{SF} between the CQI 26A compounds and the DQI **27A** compounds. Furthermore, while SF in DQI **P-27A-P** is relatively slow, it is still significantly faster than in **T-27N-T** and **P-27N-P**.

In support of the above model, we observe several peaks in the CT region of the experimental absorption spectra for both DQI **27A** and CQI **26A** bridge compounds. The relative intensities of this series of peaks vary with connectivity. For example, in the **T-27A-T** DQI compound, the dominant transition is centered near 2.95 eV, with weak shoulders offset by approximately 0.2 eV on either side of the main transition. In the CQI analog (**T-26A-T**), the main peak is reduced in intensity while the relative oscillator strength of the shoulders is increased. A more pronounced effect is observed in **PβP**, where the relative intensity of the shoulders becomes larger than the primary peak in **P-26A-P (**SI **Figure S8)**. While previous theoretical treatments of the absorption spectra in directly-bonded acene oligomers suggested that bright charge-transfer type transitions can emerge in cases of strong chromophore-chromophore coupling[37], neither the effect of the chemical bridge nor implications for the SF dynamics were considered. Here we see that both a large CT_{CC} contribution to the CT excitation and a strong transition dipole moment are essential for fast iSF. The former is a signature of direct quantum mechanical coupling between the SFCs while the latter ensures that virtual excitation of the CT excited state efficiently couples the singlet and triplet pair states (SI).[20,35] We note that while the role of virtual CT states in mediating the rate of SF has long been inferred, these data represent fundamental evidence of such an effect.[38–42]

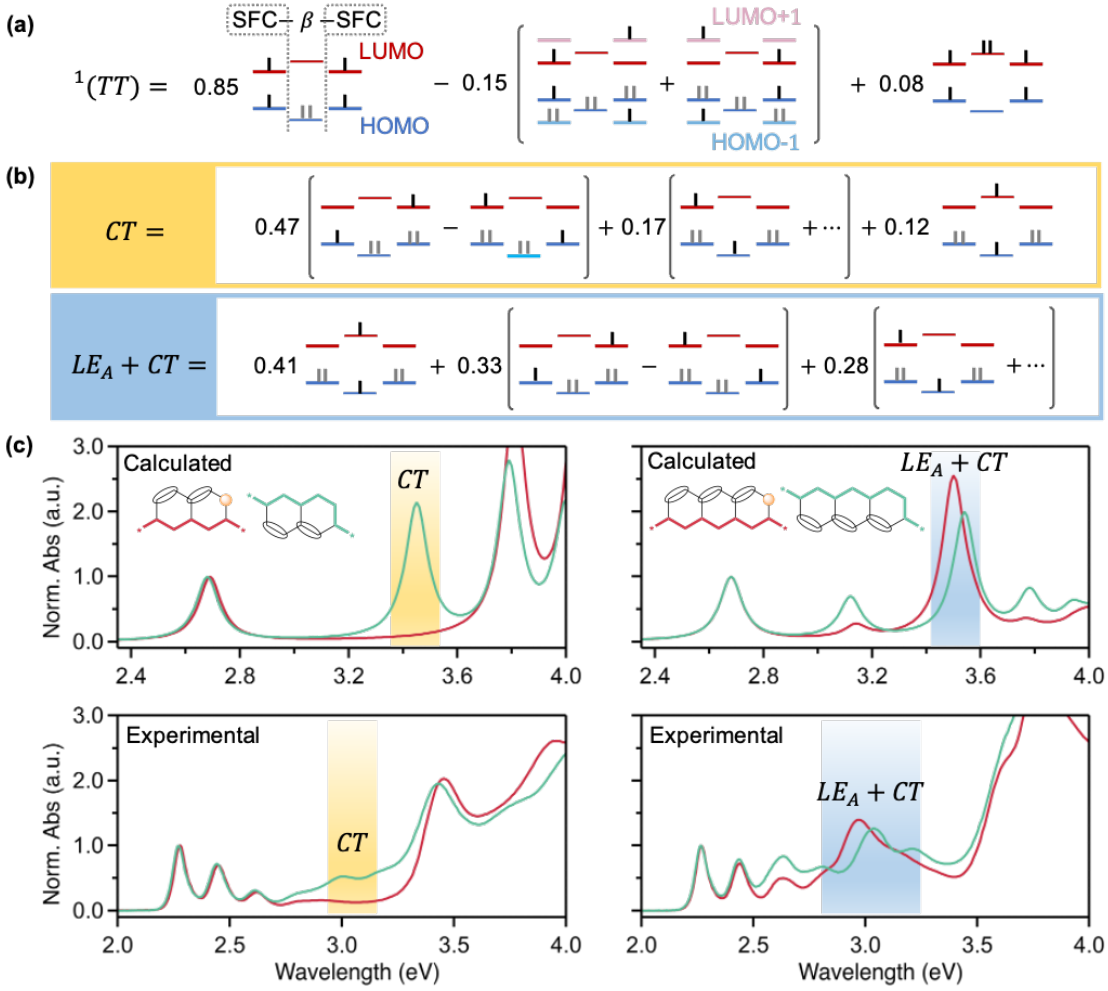

Figure 4. (a) Normalized triplet pair wavefunction for **T-26N-T** and **T-27N-T** in the molecular exciton basis representation. The overall spin is zero for each individual configuration. Bonding (antibonding) MOs not shown in any configuration are completely filled (empty). **(b)** Normalized charge transfer wavefunctions for **T-26N-T** (yellow) and **T-26A-T** (blue). The latter exhibits significant admixing with local excitation on the anthracene monomer and is labeled accordingly. Ellipses correspond to additional terms related by mirror-plane and charge-conjugation symmetries. **(c)** Calculated (top) and experimental (bottom) normalized absorption spectra for **T-N-T** (left) and **T-A-T** (right). Green traces correspond to a CQI bridge (**26N** or **26A**), red traces correspond to a DQI bridge (**27N** or **27A**). Contributions to the absorption spectra from the charge transfer wavefunctions depicted in (b) are highlighted and labeled. Calculations assume planar

conformation. The inclusion of intermonomer rotation decreases the intensity of the CT absorption but the absorption energy is largely unaffected.[32]

Table 2. Calculated energies, transition dipole couplings with the ground state, and wavefunction characteristics of charge-transfer states for PβP and TβT.

SFC	β	E (eV)	μ	CT_{CC}	$CT_{C\beta}$	LE_{β}
Tetracene	**26N**	3.45	1.67	0.47	0.17	0.12
	27N	3.55	0.06	0.57	0.14	0.08
	26A	3.54	1.61	0.33	0.28	0.41
		3.78	0.87	0.52	0.19	0.15
	27A	3.57	0.50	0.39	0.29	0.33
		3.77	0.40	0.45	0.20	0.16
Pentacene	**26N**	3.11	0.99	0.55	0.10	0.05
		3.33	0.68	0.22	0.08	0.05
	27N	3.18	0.03	0.60	0.08	0.03
		3.31	0.74	0	0.09	0.03
	26A	3.05	1.46	0.26	0.25	0.48
		3.24	0.50	0.51	0.04	0.47
		3.34	0.44	0.16	0.05	0.31
		3.54	1.65	0.16	0.30	0.39
	27A	3.11	0.37	0.24	0.25	0.55
		3.25	0.31	0.53	0.05	0.38
		3.34	0.46	0.02	0.08	0.39
		3.57	0.46	0.18	0.32	0.33

μ = transition dipole coupling with ground state (units of Å, electronic charge e = 1), CT_{CC} and $CT_{C\beta}$= normalized coefficients of configurations with CT between terminal chromophores and between terminal chromophore and bridge (β), respectively, LE_{β} = normalized coefficient of configuration with monomer excitation on the bridge molecule.

Conclusion

This work provides a new perspective on the mechanism of intramolecular singlet fission in which destructive and constructive quantum interference (QI) plays an essential role. While graphical models to predict QI based on connectivity have been successful in single-molecule electronics, these models are not as obviously applied to light-induced processes involving exciton transport in donor-bridge-acceptor systems. Here, QI graphical models successfully describe multiexciton formation as a function of connectivity in a variety of acene bridges, which is effective in part due to the symmetric nature of the iSF chromophores. Moreover, we found that both bridge resonance

contributions and structural distortion arising from steric interactions with the chromophores also impact triplet pair formation and the magnitude of QI effects. Understanding electronic structure contributions and QI to the fundamental principles of triplet pair evolution is important for optimizing the formation of entangled spin states, enhancing their utility in quantum information technologies.

Methods

Synthesis

The synthesis of pentacene and tetracene bridged dimers with β = **14Ph**, **26N**, and **26A** have been previously reported.[25,24] Similar cross-coupling conditions are used to synthesize β = **13Ph**, **27N**, **15N**, **16N**, and **27A**, as detailed in the SI. We note that TIPS (triisopropylsilylethynyl) groups are installed on all anthracene, tetracene, and pentacene chromophores for solubility and stability.

Ultrafast Spectroscopy

The iSF dynamics of the series were characterized by transient absorption spectroscopy (TAS). The protocol for identifying intramolecular SF in solution is well-established[24,43,13] (additional details provided in the SI). Briefly, a dilute solution of a compound in solution (~50 μM in toluene) is pumped by a laser pulse resonant with a vibrational excited state of the S_1 exciton. The broadband transient response is measured across the ground state bleach ($S_0 \rightarrow S_1$ transition) as well as the singlet ($S_1 \rightarrow S_n$ transition) and triplet ($T_1 \rightarrow T_n$ transition) photoinduced absorption (PIA) features. The singlet exciton on pentacene is identified by a characteristic broad PIA between 400-575 nm that decays commensurate with the rise of the triplet exciton, characterized by its narrow PIA feature peaked around 520 nm. A similar set of extensively characterized PIA features can be used to quantify the singlet to triplet formation rate in tetracene-based compounds. The assignment of triplet excitons in these compounds is verified through triplet sensitization measurements based on collisional energy transfer. Comparison of the photoexcited and sensitized triplet properties allows us to distinguish individual triplets (formed by intersystem crossing for example) from triplet pairs formed by SF. In general, the SF-generated triplet pair and individual sensitized triplet show similar transient spectra but differ markedly in their recombination dynamics, with triplet pairs exhibiting a characteristic triplet-triplet annihilation process that leads to a biexponential decay of the overall triplet population. Standard global analysis procedures are

used to obtain deconvoluted spectra and extract time constants. For all compounds used in this study, the overall SF yield is determined from kinetic arguments comparing the relative rates of singlet decay to the ground state ($S_1 \rightarrow S_0$) to decay via triplet pair formation ($S_1 \rightarrow {}^1(TT)$). Further discussion of yields can be found in the SI. Importantly, no other photoproducts are observed in this series of compounds, permitting a direct comparison of rate constants.

Quantum Chemical Calculations

The π-electron only Pariser-Parr-Pople Hamiltonian is written as[30,31]:

$$\mathcal{H} = \sum_{\langle ij\rangle,\sigma} t_{ij}\left(c_{i\sigma}^{\dagger}c_{j\sigma} + c_{j\sigma}^{\dagger}c_{i\sigma}\right) + U\sum_{i} n_{i\uparrow}\, n_{i\downarrow} + \sum_{i<j} V_{ij}\,(n_i - 1)(n_j - 1)$$

Here, $c_{i\sigma}^{\dagger}$ creates an electron with spin σ on the p_z orbital of carbon (C) atom i, $n_{i\sigma} = \sum_i c_{i\sigma}^{\dagger}\, c_{i\sigma}$ is the number of electrons with spin σ on atom i, and $n_i = \sum_\sigma n_{i\sigma}$ is the total number of electrons on the atom. We retain electronic hoppings t_{ij}only between nearest neighbors *i* and *j*. U is the Coulomb repulsion between two electrons occupying the p_z orbital of the same C-atom, and V_{ij} is long-range Coulomb interaction. The average bond lengths within an acene unit are different for the peripheral (1.40 Å) and internal (1.46 Å) bonds. Based on a widely used bond length-hopping integral relationships,[44] we have chosen intra-acene peripheral (internal) hopping integrals t_{ij} as 2.4 (2.2) eV. We have chosen planar geometries for both and therefore interunit hopping integrals 2.2 eV between the SFC monomers and the bridge molecules, although this can be relaxed .[45] We use the screened Ohno parameterization for the long-range Coulomb repulsion, $V_{ij} = U/\kappa\left[1 + 0.6117R_{ij}^2\right]^{1/2}$ where R_{ij} is the distance in Å between C-atoms *i* and *j* and κ is an effective dielectric constant.[32,33,46] Based on our previous work[47] we have chosen $U = 7.7$ eV and $\kappa = 1.3$.

Our calculations use the molecular exciton basis, with Hartree-Fock (HF) MOs localized on individual monomers.[32,46,47] Depending on the compound, we have retained between 24 to 30 exciton basis MOs, of which 4-6 are localized on the bridge molecules, with equal numbers of bonding and antibonding MOs (see SI). Further details may be found in previous studies[20,32,33,46,47] and in the SI. To arrive at the precise description of the two electron-two hole (2e-2h) ${}^1(TT)$ excitation, we use the multiple reference singles and doubles configuration interaction (MRSDCI)

approach,[33,44,48] which includes configuration interactions with the most dominant 4e-4h excitations. The total number of many-electron configurations retained to describe any single eigenstate is several million. In addition to the wavefunctions and energies, we also calculate the transition dipole couplings from the ground state to all excited states and the linear absorption spectra.

References

1. Su, T. A., Neupane, M., Steigerwald, M. L., Venkataraman, L. & Nuckolls, C. Chemical principles of single-molecule electronics. *Nat. Rev. Mater.* **1**, 16002 (2016).
2. Lambert, C. J. Basic concepts of quantum interference and electron transport in single-molecule electronics. *Chem. Soc. Rev.* **44**, 875–888 (2015).
3. Jan van der Molen, S. & Liljeroth, P. Charge transport through molecular switches. *J. Phys. Condens. Matter* **22**, 133001 (2010).
4. Guédon, C. M. *et al.* Observation of quantum interference in molecular charge transport. *Nat. Nanotechnol.* **7**, 305–309 (2012).
5. Arroyo, C. R. *et al.* Signatures of Quantum Interference Effects on Charge Transport Through a Single Benzene Ring. *Angew. Chem. Int. Ed.* **52**, 3152–3155 (2013).
6. Solomon, G. C. *et al.* Understanding quantum interference in coherent molecular conduction. *J. Chem. Phys.* **129**, 054701 (2008).
7. Tsuji, Y., Hoffmann, R., Strange, M. & Solomon, G. C. Close relation between quantum interference in molecular conductance and diradical existence. *Proc. Natl. Acad. Sci.* **113**, E413–E419 (2016).
8. Markussen, T., Stadler, R. & Thygesen, K. S. The Relation between Structure and Quantum Interference in Single Molecule Junctions. *Nano Lett.* **10**, 4260–4265 (2010).
9. Ortiz, R. *et al.* Exchange Rules for Diradical π-Conjugated Hydrocarbons. *Nano Lett.* **19**, 5991–5997 (2019).
10. Gorczak, N. *et al.* Computational design of donor-bridge-acceptor systems exhibiting pronounced quantum interference effects. *Phys. Chem. Chem. Phys.* **18**, 6773–6779 (2016).
11. Gorczak, N. *et al.* Charge transfer versus molecular conductance: molecular orbital symmetry turns quantum interference rules upside down. *Chem. Sci.* **6**, 4196–4206 (2015).

12. Sanders, S. N. *et al.* Exciton Correlations in Intramolecular Singlet Fission. *J. Am. Chem. Soc.* **138**, 7289–7297 (2016).
13. Pun, A. B. *et al.* Ultra-fast intramolecular singlet fission to persistent multiexcitons by molecular design. *Nat. Chem.* **11**, 821–828 (2019).
14. Krishnapriya, K. C. *et al.* Spin density encodes intramolecular singlet exciton fission in pentacene dimers. *Nat. Commun.* **10**, 33 (2019).
15. Sakuma, T. *et al.* Long-Lived Triplet Excited States of Bent-Shaped Pentacene Dimers by Intramolecular Singlet Fission. *J. Phys. Chem. A* **120**, 1867–1875 (2016).
16. Nakamura, S. *et al.* Enthalpy–Entropy Compensation Effect for Triplet Pair Dissociation of Intramolecular Singlet Fission in Phenylene Spacer-Bridged Hexacene Dimers. *J. Phys. Chem. Lett.* **12**, 6457–6463 (2021).
17. Korovina, N. V. *et al.* Linker-Dependent Singlet Fission in Tetracene Dimers. *J. Am. Chem. Soc.* **140**, 10179–10190 (2018).
18. Ito, S., Nagami, T. & Nakano, M. Design Principles of Electronic Couplings for Intramolecular Singlet Fission in Covalently-Linked Systems. *J. Phys. Chem. A* **120**, 6236–6241 (2016).
19. Paul, S., Govind, C. & Karunakaran, V. Planarity and Length of the Bridge Control Rate and Efficiency of Intramolecular Singlet Fission in Pentacene Dimers. *J. Phys. Chem. B* **125**, 231–239 (2021).
20. Chesler, R., Khan, S. & Mazumdar, S. Wave Function Based Analysis of Dynamics versus Yield of Free Triplets in Intramolecular Singlet Fission. *J. Phys. Chem. A* **124**, 10091–10099 (2020).

21. Abraham, V. & Mayhall, N. J. Simple Rule To Predict Boundedness of Multiexciton States in Covalently Linked Singlet-Fission Dimers. *J. Phys. Chem. Lett.* **8**, 5472–5478 (2017).
22. Herrmann, C. Electronic Communication as a Transferable Property of Molecular Bridges? *J. Phys. Chem. A* **123**, 10205–10223 (2019).
23. Walter, D., Neuhauser, D. & Baer, R. Quantum interference in polycyclic hydrocarbon molecular wires. *Chem. Phys.* **299**, 139–145 (2004).
24. Sanders, S. N. *et al.* Quantitative Intramolecular Singlet Fission in Bipentacenes. *J. Am. Chem. Soc.* **137**, 8965–8972 (2015).
25. Parenti, K. R. *et al.* Bridge Resonance Effects in Singlet Fission. *J. Phys. Chem. A* **124**, 9392–9399 (2020).
26. Davis, W. B., Svec, W. A., Ratner, M. A. & Wasielewski, M. R. Molecular-wire behaviour in p -phenylenevinylene oligomers. *Nature* **396**, 60–63 (1998).
27. Fuemmeler, E. G. *et al.* A Direct Mechanism of Ultrafast Intramolecular Singlet Fission in Pentacene Dimers. *ACS Cent. Sci.* **2**, 316–324 (2016).
28. Yablon, L. M. *et al.* Singlet fission and triplet pair recombination in bipentacenes with a twist. *Mater. Horiz.* **9**, 462–470 (2022).
29. Quinn, J. R., Foss, F. W., Venkataraman, L., Hybertsen, M. S. & Breslow, R. Single-Molecule Junction Conductance through Diaminoacenes. *J. Am. Chem. Soc.* **129**, 6714–6715 (2007).
30. Pariser, R. & Parr, R. G. A Semi-Empirical Theory of the Electronic Spectra and Electronic Structure of Complex Unsaturated Molecules. I. *J. Chem. Phys.* **21**, 466–471 (1953).
31. Pople, J. A. Electron interaction in unsaturated hydrocarbons. *Trans. Faraday Soc.* **49**, 1375 (1953).

32. Khan, S. & Mazumdar, S. Diagrammatic Exciton Basis Theory of the Photophysics of Pentacene Dimers. *J. Phys. Chem. Lett.* **8**, 4468–4478 (2017).
33. Khan, S. & Mazumdar, S. Theory of Transient Excited State Absorptions in Pentacene and Derivatives: Triplet–Triplet Biexciton versus Free Triplets. *J. Phys. Chem. Lett.* **8**, 5943–5948 (2017).
34. Smith, M. B. & Michl, J. Singlet Fission. *Chem. Rev.* **110**, 6891–6936 (2010).
35. Berkelbach, T. C., Hybertsen, M. S. & Reichman, D. R. Microscopic theory of singlet exciton fission. II. Application to pentacene dimers and the role of superexchange. *J. Chem. Phys.* **138**, 114103 (2013).
36. Kittel, C. & Fong, C. Y. *Quantum theory of solids*. (Wiley, 1987).
37. Hele, T. J. H. *et al.* Anticipating Acene-Based Chromophore Spectra with Molecular Orbital Arguments. *J. Phys. Chem. A* **123**, 2527–2536 (2019).
38. Beljonne, D., Yamagata, H., Brédas, J. L., Spano, F. C. & Olivier, Y. Charge-Transfer Excitations Steer the Davydov Splitting and Mediate Singlet Exciton Fission in Pentacene. *Phys. Rev. Lett.* **110**, (2013).
39. Basel, B. S. *et al.* Evidence for Charge-Transfer Mediation in the Primary Events of Singlet Fission in a Weakly Coupled Pentacene Dimer. *Chem* **4**, 1092–1111 (2018).
40. Busby, E. *et al.* A design strategy for intramolecular singlet fission mediated by charge-transfer states in donor–acceptor organic materials. *Nat. Mater.* **14**, 426–433 (2015).
41. He, G. *et al.* Charge transfer states impact the triplet pair dynamics of singlet fission polymers. *J. Chem. Phys.* **153**, 244902 (2020).
42. Monahan, N. & Zhu, X.-Y. Charge Transfer–Mediated Singlet Fission. *Annu. Rev. Phys. Chem.* **66**, 601–618 (2015).

43. Kumarasamy, E. *et al.* Tuning Singlet Fission in π-Bridge-π Chromophores. *J. Am. Chem. Soc.* **139**, 12488–12494 (2017).
44. Aryanpour, K., Shukla, A. & Mazumdar, S. Theory of Singlet Fission in Polyenes, Acene Crystals, and Covalently Linked Acene Dimers. *J. Phys. Chem. C* **119**, 6966–6979 (2015).
45. Ramasesha, S., Albert, I. D. L. & Sinha, B. Optical and magnetic properties of the exact PPP states of biphenyl. *Mol. Phys.* **72**, 537–547 (1991).
46. Khan, S. & Mazumdar, S. Optical probes of the quantum-entangled triplet-triplet state in a heteroacene dimer. *Phys. Rev. B* **98**, 165202 (2018).
47. Chandross, M. & Mazumdar, S. Coulomb interactions and linear, nonlinear, and triplet absorption in poly(para-phenylenevinylene). *Phys. Rev. B* **55**, 1497–1504 (1997).
48. Tavan, P. & Schulten, K. Electronic excitations in finite and infinite polyenes. *Phys. Rev. B* **36**, 4337–4358 (1987).

Acknowledgements

This material is based upon work supported by the U.S. Department of Energy, Office of Science, Office of Basic Energy Sciences under Award Number DE-SC0022036 and the National Science Foundation under Award Number CHE-1764152. K.R.P. thanks the Department of Defense for a National Defense Science and Engineering (NDSEG) Fellowship. J.Z. thanks the Columbia College Science Scholars Program and Guthikonda Fellowship. X.Y. acknowledges the Beijing Institute of Technology Research Fund Program for Young Scholars, and the Analysis and Testing Center of Beijing Institute of Technology for NMR and MS characterization. This research used resources at the Center for Functional Nanomaterials, which is a U.S. DOE Office of Science Facility at Brookhaven National Laboratory under contract DE-SC0012704.

Author Contributions

S.M., M.Y.S and L.M.C. oversaw the project. K.R.P., M.Y.S. and L.M.C. designed the molecules. G.H. collected transient absorption spectroscopy data and K.R.P., G.H. and M.Y.S. carried out data analysis. K.R.P., B.X., D.M., and J.Z. synthesized and characterized the molecules, supervised by X.Y. and L.M.C. Theory models were designed by S.M. and A.S. Pariser-Parr-Pople calculations were carried out by R.C. and P.B. DFT calculations were carried out by G.H. The paper was written by K.R.P., S.M., M.Y.S. and L.M.C. with contributions from all authors.

Competing Interests

The authors declare no competing financial interests.

Additional Information

Supplementary Information

- Experimental and computational details, synthetic characterization, transient absorption spectra and global analysis, DFT geometry calculations, NMR spectra